



The author(s) shown below used Federal funding provided by the U.S. Department of Justice to prepare the following resource:

Document Title: The Application of Gold Nanoparticles for the Trace Detection of Synthetic Cannabinoids in Saliva and Urine by Surface Enhanced Raman Spectroscopy

Author(s): Bruce McCord, Ph.D.

Document Number: 254675

Date Received: April 2020

Award Number: 2015-IJ-CX-K006

This resource has not been published by the U.S. Department of Justice. This resource is being made publically available through the Office of Justice Programs' National Criminal Justice Reference Service.

Opinions or points of view expressed are those of the author(s) and do not necessarily reflect the official position or policies of the U.S. Department of Justice.

The Application of Gold Nanoparticles for the Trace Detection of Synthetic Cannabinoids in Saliva and Urine by Surface Enhanced Raman Spectroscopy

Bruce McCord, Ph.D

Florida International University

11200 SW 8th Street CP 304

Miami, FL 33199

305-348-7543

mccordb@fiu.edu

Federal Agency: National Institute of Justice

Grant Number: NIJ 2015-IJ-CX-K006

Submission date: September 19, 2019

Recipient Organization: Florida International University

11200 SW 8th Street Miami, FL 33199

Submitting Official: Mr. Roberto Gutierrez

Assistant Vice President for Research

Office of Research and Economic Development

11200 SW 8th Street, MARC 430

Miami, Florida, 33199

305-348-2494

gutierr@fiu.edu

Signature of Submitting Official:



JT

A. Introduction

The use and abuse of synthetic cannabinoids has increased significantly in recent years due to their easy access and growing popularity in young adults. This popularity has led to a concomitant increase in emergency room visits due to synthetic cannabinoid intoxication.¹⁻³ As more of these drugs become illegal, new legal analogs of these drugs are being made. This presents problems for the hospitals and the forensic investigators as standard methods may not detect the target drug.

The most common methods of screening for drugs of abuse in biological samples are based on immunoassays.⁴ However, these methods are based on bio-recognition elements, and thus they are sensitive to the molecular structure and geometry of the target analyte, making them intrinsically prone to loss of specificity across drug analog generations.

A potential solution to this issue is Surface Enhanced Raman Spectroscopy (SERS). When Raman spectroscopy is performed in the presence of plasmonic nanostructures, the signal can be enhanced by several orders of magnitude via the excitation of the localized surface plasmon resonance (LSPR). This generates an electromagnetic field at the nanostructure surface that is much stronger than the one generated by the impinging Raman laser source, thus allowing the detection of trace analytes.⁵ The creation of hot-spots due to the addition of aggregating agents further contributes to the enhancement of the signal.⁶ This method has already been demonstrated to work for the toxicological detection of benzodiazepines in urine with limits of detection ranging from 1 to 200 ng/mL.^{7,8} As a screening technique, surface enhanced Raman spectroscopy presents some unique advantages. It is fast, sensitive, and provides an approach towards structural elucidation that is orthogonal to traditional chromatographic-mass spectrometric techniques. Furthermore, because the detection system is relatively generic, newly synthesized compounds can easily be added to existing libraries without extensive modification or development of new procedures.

B. JWH-018 as model synthetic cannabinoid. Fundamental spectroscopic work towards *in-silica* library building

JWH-018 is a naphthoylindole synthetic cannabinoid (*Figure 8.1*, left panel) and it has been chosen as the model analyte because it is among the first to be designated as a Schedule I substance by the DEA⁹ as well as one of the most studied synthetic cannabinoids in terms of toxicological concentrations in humans and metabolic behavior.¹⁰⁻¹³ Due to the lack of in-depth spectroscopic studies on it, DFT calculations were used as a tool to identify the most stable molecular geometry and interpret vibrational modes. An in-depth study of the adsorption behavior on citrate-capped gold nanospheres was also addressed.

DFT calculations involved geometry optimization and calculation of Raman frequencies, and were performed using Gaussian 09 with the B3LYP hybrid exchange correlation functional and 6-311G** basis set.¹⁴ DFT Raman frequencies of JWH-018 were scaled by a factor of 0.9779, which was obtained according to standard least-squares minimization procedure over the 1800-200 cm⁻¹ range of interest.¹⁵ The simulated Raman spectrum is reported in the central panel of *Figure 8.1*, together with the experimental normal Raman spectrum of solid state JWH-018. To assess the level of agreement between the theoretical and experimental frequencies obtained in normal Raman setting, the absolute and percent error for each scaled theoretical-experimental frequency pair have been calculated.¹⁶ Overall, the small number (3) of notable absolute error values, together with a percent error of predicted-experimental pairs that never exceeds 1.6% within the selected spectral range, denotes an excellent agreement of the predicted frequencies with the experimental data.¹⁶

It would be lengthy for the analyst if this procedure had to be repeated for each studied compound belonging to the same chemical class. For this reason, we explored whether the scaling factor calculated on the basis of JWH-018 experimental-theoretical pairs (A 0.9779) could be successfully applied to correct the simulated spectra of other molecules belonging to the synthetic cannabinoids class. In our studies, the JWH-018-based scaling factor was found to be appropriate for other synthetic cannabinoids belonging to different sub-classes (*Table 8.1*). The calculated error metrics show excellent agreement between predicted and experimental data, making the utilized computational method and scaling factor very promising for *in silico* database building.

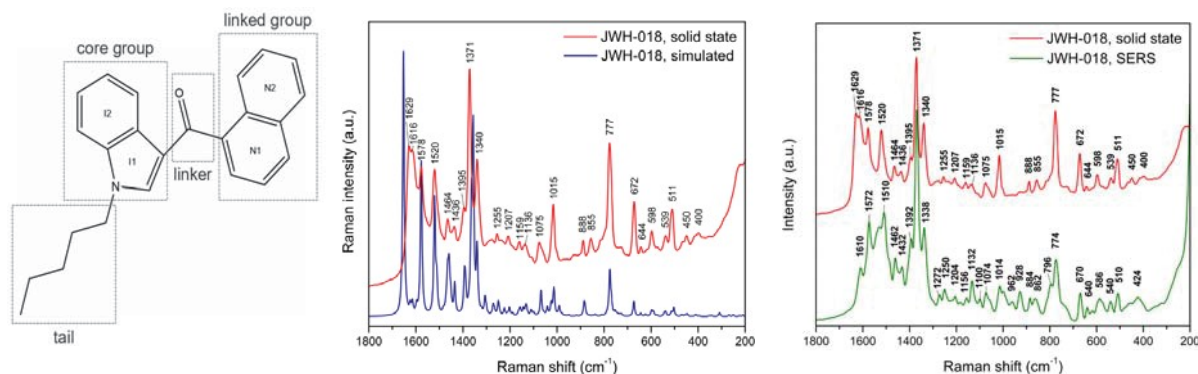


Figure B.1. Structure of JWH-018 with highlighted synthetic cannabinoids' nomenclature (*left*); comparison between DFT-simulated (bottom, blue) and experimental (top, red) Raman spectra of JWH-018 (*center*); Comparison of SERS spectrum of JWH-018 standard methanolic solution at a concentration of 1000 ng/mL (bottom, green) with normal Raman spectrum of JWH-018 in the solid state (top, red). Intensities are on the same scale, and spectra have been stacked for ease of comparison. (*right*).

Table B.1. Summary of percent error metrics for the synthetic cannabinoids added so far to the *in silico* database.

compound	class	subclass	maximum %error	average %error
JWH-018	indole	naphthoylindole	1.6%	0.47%
JWH-081	indole	naphthoylindole	3.1%	0.53%
JWH-175	indole	naphthylmethylindole	6.5%	0.70%
JWH-250	indole	phenylacetylindole	2.4%	2.4%
RCS-4	indole	benzoylindole	1.6%	0.46%
XLR-11	indole	tetramethylcyclopropylindole	5.1%	1.0%
ADB-PINACA	indazole	indazolamide	4.8%	1.1%

When evaluating the potential of SERS as a fit-to-purpose technique for forensic toxicology applications, it is important to quantify the affinity between the target analyte and the enhancing substrate. This will dictate whether a method developed for standard solutions will adequately perform once translated to analytes in matrix, as matrix components may compete for adsorption sites and hinder the signal of interest.¹⁷ The affinity between JWH-018 and the citrate-reduced gold nanoparticle substrate was quantified by studying their adsorption behavior.¹⁶ As shown in *Figure 8.2*, this can be fitted to a Langmuir adsorption model, which allows for the extrapolation of the adsorption constant K_{ad} .^{16,18}

$$i = \frac{I_{sat}K_{ad}[JWH-018]_i}{1+K_{ad}[JWH-018]_i} \quad \{Equation 8.1\}$$

where I_i is the SERS intensity at the i th concentration point, I_{sat} is the SERS intensity at saturation, and $[JWH-018]_i$ is the i th molar concentration of the adsorbed drug. The extrapolated K_{ad} is $9.3 \times 10^6 \pm 1.2 \text{ L}\cdot\text{mol}^{-1}$. From a qualitative point of view, the observed Langmuir behavior in conjunction with the obtained value of K_{ad} demonstrate a high affinity of JWH-018 for the colloidal gold substrate. More specifically, the affinity is higher than the strength of the intermolecular forces existing among individual drug molecules. This has positive consequences on the sensitivity of the analytical method, as in a SERS experiment the stronger the interaction between the analyte and the substrate, the greater the enhancement of the scattered Raman signal, and the lower the detection limit. The thermodynamic derivation of K_{ad} ¹⁹ was then used to determine the free energy for the adsorption of JWH-018 on the citrate-reduced colloidal gold nanospheres. The value of ΔG^0 for the adsorption process was calculated to be $-39.2 \pm 2.9 \text{ kJ/mol}$, indicating a spontaneous process. Both ΔG^0 and K_{ad} are the same order of magnitude as what was reported in the literature for thiol- and thione-containing analytes,²⁰ which are SERS reporters that strongly adsorb on gold,^{21,22} strengthening the argument for high affinity to the gold nanoparticles. Aromatic compounds are indeed found to strongly interact with gold nanoparticles, included citrate-capped nanospheres, on which they are thought to adsorb by either citrate displacement or reorientation.^{23,24}

The low surface coverage limit of Equation 8.1 was used to characterize the sensitivity of the method.^{16,18} The calculated LOD was 0.8 ng/mL (2×10^{-9} M),¹⁶ indicating high sensitivity and reflecting what was deduced by the high adsorption constant K_{ad} . This LOD is of the same order of magnitude found in current immunoassays methods utilized for synthetic cannabinoids in oral fluid.²⁵ This level of sensitivity is also compatible with the toxicological levels of synthetic cannabinoids reported for impaired individuals,¹² thus this procedure should be useful for drug detection in emergency room settings. Other analytical figures of merit such as the LOQ ($10a_{noise}$ method blank) are reported in Table 8.2.

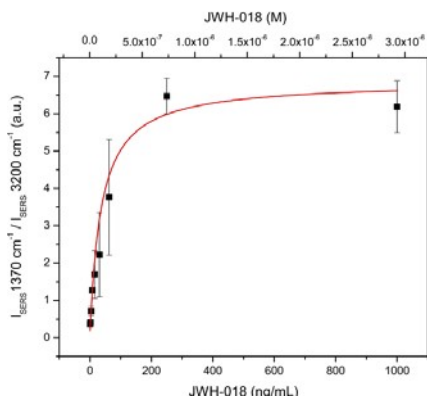


Figure B.2. Adsorption isotherm of JWH-018 on traditional citrate-reduced gold nanospheres. The Langmuir fitting (adjusted R^2 0.974) is shown in red.

Table B.2. Analytical figures of merit for JWH-018 in standard solution

Analytical Enhancement Factor ²⁶	1.3×10^5
LOD	0.8 ng/mL (2×10^{-9} M)
LOQ	2 ng/mL (7×10^{-9} M)
Dynamic range	2.0 - 7.8 ng/mL ($7.0 - 2.5 \times 10^{-9}$ M)
Limit of linearity	16 ng/mL (5.0×10^{-8} M)
a_{noise} method blank (1368 - 1374 cm^{-1})	0.04 a.u.
Selectivity (slope of calibration curve)	0.142 ± 0.007
Standard Error of calibration curve	1 ng/mL

C. Optimization of gold nanoparticle aggregation conditions and translation of detection method to a portable Raman platform

Analysis of understanding the nanoparticle and aggregating agent interaction for SERS method optimization has been conducted focusing on the effect of monovalent (K^+ and Na^+), divalent (Ca^{2+} and Mg^{2+}), and trivalent (Al^{3+}) chloride, sulfate and nitrate salts and assessing at what concentration aggregation occurs for each salt and how the UV-VIS absorption spectra, nanoparticle size, and zeta potential of the nanoparticles change with the addition of the aggregating agent.

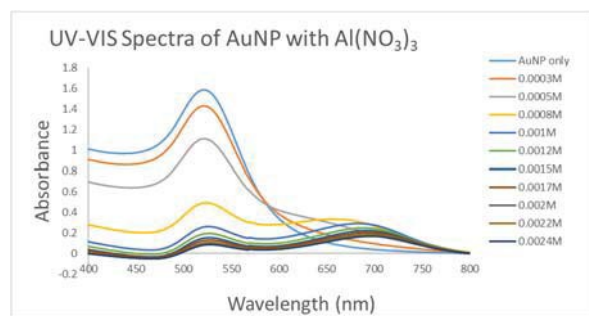


Figure C1. Characterization of the changes in absorption of the gold nanoparticle solution as concentration of $Al(NO_3)_3$ increases.

In the UV-Vis study, various aggregating agents were titrated into the gold nanoparticle solution and the change in the absorbance of the gold nanoparticles was documented. As aggregating agent concentration increased, a color transition was seen (red to purple to grey). The concentration of each aggregating agent for each color change was calculated. Three things can be concluded from the UV-vis study. First, as concentration of the aggregating agent increase the peak absorbance decreased (Figure C1). Second, trivalent cations need a lower concentration to produce aggregating in comparison divalent and monovalent cations. Third, the anion does is not the only influence aggregation. it seems that the cation could have more of an effect on nanoparticle aggregation than noted in the previous literature, which focuses on the effect of the anion as a major contributor to the detection of a compound via the SERS mechanism.

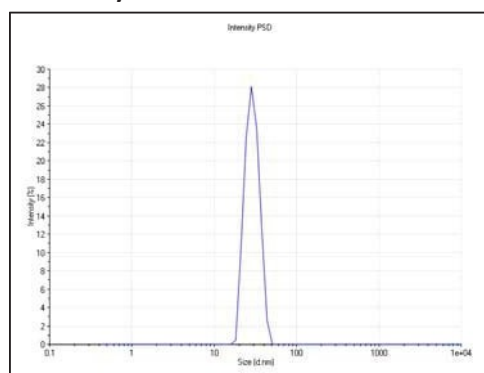
To further study the nanoparticle aggregating agent interaction, a zetasizer was used to assess the change in nanoparticle size and zeta potential with an increase in aggregating agent concentration. The three concentrations chosen were based upon the change in color of the nanoparticle solution leading to aggregation: lowest concentration (nanoparticle solution color stayed red), middle concentration (purple color change), highest concentration (grey color change). This study was split into two parts: [1] the change in zeta potential and nanoparticle size with the initial addition of the aggregating agent (980 μ L AuNP + 10 μ L aggregating agent) and [2] the effect on zeta potential and nanoparticle size with the SERS study negative control (980 μ L AuNP + 10 μ L aggregating agent + 10 μ L of 10% methanol). All synthetic cannabinoids examined were in a 10% methanol solution, prior to being added to the nanoparticle solution containing the aggregating agent.

From this study, multiple conclusions can be made. First, for a majority of the aggregating agents, as the salt concentration increased the average nanoparticle size increases (*Table C1*). This is as expected, since the addition of the salt destabilizes the nanoparticles to bring them closer together simulating a larger nanoparticle size. Second, as the aggregating agent is added to the nanoparticles the single peak splits into two peaks and reforms as one peak at the concentration that aggregation occurs (*Figure C2*). This is a great visual representation showing the amount of the nanoparticles that aggregate with a given aggregating agent concentration.

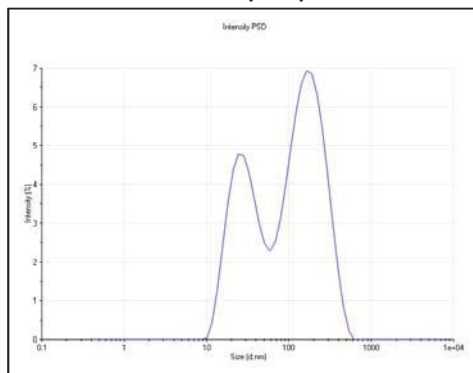
Salt Concentration	AuNP Size Avg (nm)	AuNP Size Std Dev
None	27.7	6.7
0.0084M NaCl	51.9	14
0.033M NaCl	130	51
0.048M NaCl	130	18
0.00025M CaCl ₂	41.5	4.3
0.00075M CaCl ₂	132	48
0.001M CaCl ₂	138	18
0.00025M MgCl ₂	31.1	5.8
0.00075M MgCl ₂	87.9	37
0.0015M MgCl ₂	164	44
0.00025M AlCl ₃	56.1	12
0.0005M AlCl ₃	46.5	11
0.0012M AlCl ₃	129	24

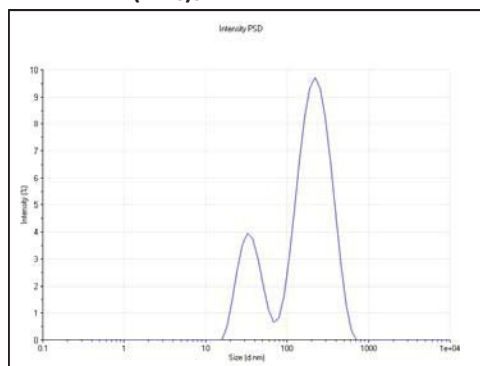
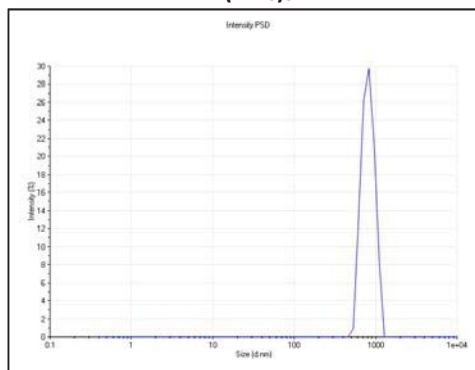
Table C1. An assessment of the change in nanoparticle size with an increase in aggregating agent concentration.

AuNP Only



0.00025M Al(NO₃)₃



0.0005M Al(NO₃)₃**0.001M Al(NO₃)₃****Figure C2.** An assessment of the change in nanoparticle size with an increase in NaNO₃ aggregating agent concentration.

Third, with the addition of monovalent, divalent and trivalent salts the zeta potential decreases as the concentration of the salt increases for the sulfate and nitrate salts. However, despite having a higher concentration of chloride ions, monovalent salts show an increase in zeta potential (*Table C2*). Divalent and trivalent cations are interacting differently and producing earlier aggregation and higher zeta potentials. The decrease in the zeta potential as the aggregating agent concentration increases is expected, which destabilizes the nanoparticles for SERS enhancement. Fourth, with or without the addition of 10 μ L of 10% (0.02M) methanol, the same trends in the zeta potential are seen (*Table C2*). This is as expected. Based upon the above results, it is shown that the different salts will react to the nanoparticles differently.

Salt and Concentration	No MeOH Added		MeOH Added	
	Zeta Potential Average	Zeta Potential Standard Dev	Zeta Potential Average	Zeta Potential Standard Dev
None	-35.9	2.1	-35.1	3.8
0.0084M NaCl	-34.8	5.8	-38.6	2.6
0.033M NaCl	-46.4	4.9	-52.9	6.2
0.048M NaCl	-30.0	7.2	-34.1	3.1
0.00025M CaCl ₂	-30.5	1.8	-31.9	1.8
0.00075M CaCl ₂	-25.6	1.3	-24.3	0.8
0.001M CaCl ₂	-18.7	0.7	-21.0	1.7
0.00025M MgCl ₂	-34.6	2.2	-30.8	1.5
0.00075M MgCl ₂	-26.7	1.1	-27.1	0.9
0.0015M MgCl ₂	-22.3	1.0	-21.7	1.0
0.00025M AlCl ₃	-36.2	4.3	-36.5	3.2
0.0005M AlCl ₃	-32.7	4.1	-31.3	3.2
0.0012M AlCl ₃	-18.3	3.3	-19.6	5.2

Table C2: An assessment of the change in zeta potential with monovalent, divalent, and trivalent cations comparing chloride salts with and without the addition of 10% (0.02M) Methanol solution.

Upon understanding of the gold nanoparticle and aggregating agent interaction, nine different synthetic cannabinoids were analyzed via SERS using the previously noted salts. The SERS spectrum produced varied depending upon the salt used. For many of the salt examined, the SERS spectrum of the sample containing the synthetic cannabinoid could not be differentiated from the negative control (980 μ L AuNP + 10 μ L salt + 10 μ L of 10% (0.02M) Methanol). Limits of detection were calculated for salts used that could detect the synthetic cannabinoid examined (*Table C3*). Based upon the results, 0.0015M MgCl₂ was determined to be the optimal aggregating agent

with LODs ranging from 20-130 ng/mL. Therefore, 0.0015M MgCl₂ will be used as the aggregating agent for studied on the detection of synthetic cannabinoids in oral fluid and urine.

Drug	Aggregating Agent	Slope	Standard Deviation	R ²	LOD (ng/mL)
JWH-018	CaCl ₂	0.00007	0.025	0.75	1090
	MgCl ₂	0.0007	0.0005	0.89	20
JWH-030	MgCl ₂	0.0005	0.011	0.99	68
	AlCl ₃	0.000007	0.008	0.96	3313
JWH-073	NaCl	0.00001	0.0007	0.94	221
	MgCl ₂	0.0007	0.03	0.98	130
JWH-081	NaCl	0.000005	0.0005	0.83	328
	MgCl ₂	0.0018	0.040	0.94	66
JWH-122	MgCl ₂	0.0018	0.023	0.97	38
	AlCl ₃	0.00003	0.0058	0.98	583
JWH-147	MgCl ₂	0.0031	0.091	0.89	88
	AlCl ₃	0.000003	0.0003	0.94	266
JWH-175	CaCl ₂	0.0003	0.028	0.83	746
	MgCl ₂	0.0018	0.019	0.95	30
MAM-2201	MgCl ₂	0.0009	0.008	0.95	27
	AlCl ₃	0.000004	0.0007	0.98	554
AM-2201	NaCl	0.000006	0.00007	0.96	334
	MgCl ₂	0.001	0.038	0.99	113
	AlCl ₃	0.00002	0.010	0.91	1463

Table C3. Calculated slope, standard deviation, R², and limits of detection for nine different synthetic cannabinoids examined.

D. Development of a rapid extraction process for the detection of synthetic cannabinoids in oral fluid

Oral fluid is mainly composed of water, with proteins making up only 0.3% of its mass.²⁷⁻²⁹ This low protein content implies protein binding in oral fluid is negligible compared to blood, and target compounds, if present, can be assumed to mainly exist as free drugs.²⁷ Moreover, the oral cavity is not a typical site of xenobiotic metabolism, leading to a higher concentration of the parent compound over possible metabolites.³⁰ These facts enable screening tests based on oral fluid analysis to be targeted at the sole parent drug, constituting an advantage when analyzing NPS's, as their metabolic species are often unknown or not fully elucidated.

Although oral fluid is mainly composed of water, the small fraction of non-water components is sufficient to interfere with SERS analysis. This has been previously reported in the literature, and attributed to the presence of salivary mucins and thiocyanate.^{31,32} In order to desalt and minimize the protein fraction of fortified oral fluid samples, a two-step clean-up procedure has been implemented.¹⁶ This was constituted by a preliminary protein crashing produced in the presence of methanol, followed by a micro-solid phase extraction (μ -SPE) using commercially available miniaturized C₁₈ cartridges mounted inside 10 μ L pipette tips. This μ -SPE procedure is performed in only 4 minutes, making it a quick and easy to use clean-up method. The extracts of fortified oral fluid samples prepared with increasingly lower JWH-018 content were then used to assess the sensitivity of the method on simulated samples. A summary of the spectral profiles obtained from these extracts is reported in the left panel of *Figure 0.1*, where the SERS profile of the matrix blank is also shown. The LOD for JWH-018 in fortified oral fluid extracts is 31 ng/mL (*Table 0.1*).¹⁶

Table D.1. Analytical figures of merit for JWH-018 in fortified oral fluid samples

LOD in fortified oral fluid	31 ng/mL (7.7 x 10 ⁻⁸ M)
noise method blank (1368 - 1374 cm ⁻¹)	0.04 a.u.
Recovery	64.4%

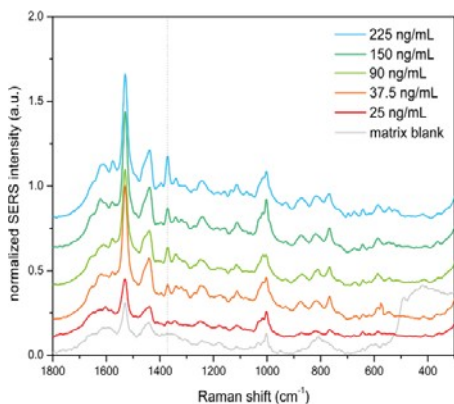


Figure D.1. SERS spectra obtained from fortified oral fluid extracts at different initial concentration of JWH-018. The SERS spectrum of the matrix blank is reported in grey. The vertical dotted line marks the drug's reference band at 1370 cm^{-1} assigned to the $\nu(\text{C}=\text{C})$ of the naphthalene moiety.

E. Development of a rapid extraction process for the detection of synthetic cannabinoids in urine

Work has begun on the on the detection of synthetic cannabinoids in spiked urine samples via SERS. Supported liquid extraction (SLE) has been examined as a fast extraction technique (20 minutes) to help remove any interferences and detect the compound of interest. In the initial study, spiked urine samples were diluted 1:1 with water or diluted 1:1 with buffer (100 mM NH_4OAc buffer solution adjusted to pH 4 with 1% formic acid). After dilution, samples were placed into the SLE+ column, washed with dichloromethane, eluted under vacuum, dried down and reconstituted with 10% (0.02M) methanol. Results show that the Raman spectrum produced was not the same as the results in the initial study. This is due to the extraction process. Therefore, adjusting the current buffer pH or concentration as well as using other buffers and organic solvents will be examined to determine the optimal SLE method for the detection of synthetic cannabinoids in urine.

F. Conclusions

Unlike standard current immuno-based procedures, SERS allows for the acquisition of a molecular fingerprint of the detected compound. As such, it could be better suited to address the analytical challenges associated with the detection of emerging psychoactive substances, as well as complement molecular confirmatory techniques such as mass spectrometry. Moreover, when compared to immunoassay-based protocols, the SERS approach is significantly faster. For example, the method developed for oral fluid samples accounts for 36 minutes of total analysis time (from sample preparation to spectral acquisition)¹⁶, as opposed to the 120 minutes reported for ELISA methods designed for the same analyte.²⁵ Due to the detection capabilities at drug concentrations commonly found in oral fluid when the effects of the substance are present,¹² we believe our protocol could be useful in emergency room settings that require quick detection of JWH-018 and other synthetic cannabinoids. Indeed, the detection of a variety of synthetic cannabinoids, both as standard solutions and as fortified urine samples, has been demonstrated by our group using the same type of SERS enhancing substrate and aggregation approach.³³ The results obtained utilizing our computational approach show high potential for building an *in silico* database for synthetic cannabinoids. This is extremely important both for seized drug identification using portable Raman spectroscopy and toxicological screening tests based on SERS. Due to the rapidity at which new analogs are developed and introduced into the market, research on novel psychoactive substances is often dependent, and thus slowed down, by the necessary time to produce commercially available analytical standards. *In silico* generated data can aid in the expansion of existing traditional spectral databases when reference materials are not available for purchase, and thus, assist in the process of keeping analytical laboratories and spectral libraries up to date with current drug usage trends.

G. References

- (1) Paul, A. B. M.; Simms, L.; Amini, S.; Paul, A. E. Teens and Spice: A Review of Adolescent Fatalities Associated with Synthetic Cannabinoid Use. *J. Forensic Sci.* **2018**, *63* (4), 1321-1324.
- (2) Trecki, J.; Gerona, R. R.; Schwartz, M. D. Synthetic Cannabinoid-Related Illnesses and Deaths. *N. Engl. J. Med.* **2015**, *373* (2), 103-107.
- (3) Labay, L. M.; Caruso, J. L.; Gilson, T. P.; Phipps, R. J.; Knight, L. D.; Lemos, N. P.; McIntyre, I. M.; Stoppacher, R.; Tormos, L. M.; Weins, A. L.; et al. Synthetic Cannabinoid Drug Use as a Cause or Contributory Cause of Death. *Forensic Sci. /nt.* **2016**, *260*, 31-39.
- (4) Smith, M. L. Immunoassay. In *Principles of Forensic Toxicology*; Levine, B., Ed.; AACC Press: Washington DC, 2010; pp 119-139.
- (5) LeRu, E. C.; Etchegoin, P. *Principles of Surface-Enhanced Raman Spectroscopy*; Elsevier, 2009.
- (6) Aroca, R. *Surface-Enhanced Vibrational Spectroscopy*; John Wiley & Sons, Ltd: Chichester, UK, 2006.

- (7) Doctor, E. L.; McCord, B. The Application of Supported Liquid Extraction in the Analysis of Benzodiazepines Using Surface Enhanced Raman Spectroscopy. *Talanta* **2015**, *144*, 938-943.
- (8) Doctor, E. L.; McCord, B. Comparison of Aggregating Agents for the Surface-Enhanced Raman Analysis of Benzodiazepines. *Analyst* **2013**, *138* (20), 5926.
- (9) DEA Moves to Emergency Control Synthetic Marijuana <https://www.dea.gov/pubs/pressrel/pr112410.html> (accessed Jun 18, 2018).
- (10) Coulter, C.; Garnier, M.; Moore, C. Synthetic Cannabinoids in Oral Fluid. *J. Anal. Toxicol.* **2011**, *35* (7), 424-430.
- (11) Su, M. K.; Seely, K. A.; Moran, J. H.; Hoffman, R. S. Metabolism of Classical Cannabinoids and the Synthetic Cannabinoid JWH-018. *Clin. Pharmacol. Ther.* **2015**, *97* (6), 562-564.
- (12) Toennes, S. W.; Geraths, A.; Pogoda, W.; Paulke, A.; Wunder, C.; Theunissen, E. L.; Ramaekers, J. G. Pharmacokinetic Properties of the Synthetic Cannabinoid JWH-018 in Oral Fluid after Inhalation. *Drug Test. Anal.* **2017**, No. September 2017, 644-650.
- (13) Cooper, Z. D.; Poklis, J. L.; Liu, F. Methodology for Controlled Administration of Smoked Synthetic Cannabinoids JWH-018 and JWH-073. *Neuropharmacology* **2018**, *134* (April 2017), 92-100.
- (14) Frisch, M. J.; Trucks, G. W.; Schlegel, H. B.; Scuseria, G. E.; Robb, M. A.; Cheeseman, J. R.; Scalmani, G.; Barone, V.; Mennucci, B.; Petersson, G. A.; et al. Gaussian 09, Revision B.01. Gaussian, Inc.: Wallingford 2010.
- (15) Scott, A. P.; Radom, L. Harmonic Vibrational Frequencies: An Evaluation of Hartree-Fock, Møller-Plesset, Quadratic Configuration Interaction, Density Functional Theory, and Semiempirical Scale Factors. *J. Phys. Chem.* **1996**, *100* (41), 16502-16513.
- (16) Deriu, C.; Conticello, I.; Mebel, A. M.; McCord, B. Micro Solid Phase Extraction Surface-Enhanced Raman Spectroscopy (μ -SPE/SERS) Screening Test for the Detection of the Synthetic Cannabinoid JWH-018 in Oral Fluid. *Anal. Chem.*
- (17) Deriu, C.; Paudyal, J.; Bhardwaj, V.; McCord, B. SERS for the Forensic Toxicological Screening of Drugs. In *Surface-Enhanced Raman Spectroscopy: Methods, Analysis and Research*; Bhardwaj, V., McGoron, A. J., Eds.; Nova Science Publishers: Hauppauge, NY.
- (18) Izquierdo-Lorenzo, I.; Sanchez-Cortes, S.; Garcia-Ramos, J. V. Adsorption of Beta-Adrenergic Agonists Used in Sport Doping on Metal Nanoparticles: A Detection Study Based on Surface-Enhanced Raman Scattering. *Langmuir* **2010**, *26* (18), 14663-14670.
- (19) Liu, Y. Is the Free Energy Change of Adsorption Correctly Calculated? *J. Chem. Eng. Data* **2009**, *54* (7), 1981-1985.
- (20) Ansar, S. M.; Haputhanthri, R.; Edmonds, B.; Liu, D.; Yu, L.; Sygula, A.; Zhang, D. Determination of the Binding Affinity, Packing, and Conformation of Thiolate and Thione Ligands on Gold Nanoparticles. *J. Phys. Chem. C* **2011**, *115* (3), 653-660.
- (21) Le Ru, E. C.; Etchegoin, P. G. *Principles of Surface-Enhanced Raman Spectroscopy and Related Plasmonic Effects*; Elsevier: Amsterdam, 2009.
- (22) Pakiari, A. H.; Jamshidi, Z. Nature and Strength of MS Bonds (M = Au, Ag, and Cu) in Binary Alloy Gold Clusters. *J. Phys. Chem. A* **2010**, *114* (34), 9212-9221.
- (23) Farkas, J.; Nizzetto, L.; Thomas, K. V. Science of the Total Environment The Binding of Phenanthrene to Engineered Silver and Gold Nanoparticles. *Sci. Total Environ.* **2012**, *425*, 283-288.
- (24) Wang, H.; Campiglia, A. D. Determination of Polycyclic Aromatic Hydrocarbons in Drinking Water Samples by Solid-Phase Nanoextraction and High-Performance Liquid Chromatography. **2008**, *80* (21), 8202-8209.
- (25) Rodrigues, W. C.; Catbagan, P.; Rana, S.; Wang, G.; Moore, C. Detection of Synthetic Cannabinoids in Oral Fluid Using ELISA and LC-MS-MS. *J. Anal. Toxicol.* **2013**, *37* (8), 526-533.
- (26) LeRu, E. C.; Meyer, M.; Etchegoin, P. G.; Le Ru, E. C.; Blackie, E. Surface Enhanced Raman Scattering Enhancement Factors: A Comprehensive Study. *J. Phys. Chem. C* **2007**, *111* (37), 13794-13803.
- (27) Drummer, O. H. Drug Testing in Oral Fluid. *Clin. Biochem. Rev.* **2006**, *27* (3), 147-159.
- (28) Chojnowska, S.; Baran, T.; Wilinska, I.; Sienicka, P.; Cabaj-Wiater, I.; Knas, M. Human Saliva as a Diagnostic Material. *Adv. Med. Sci.* **2018**, *63* (1), 185-191.
- (29) Elmongy, H.; Abdel-Rehim, M. Saliva as an Alternative Specimen to Plasma for Drug Bioanalysis. A Review. *TrAC - Trends Anal. Chem.* **2016**, *83*, 70-79.
- (30) D'Elia, V.; Garcia, G. M.; Ruiz, C. G. Spectroscopic Trends for the Determination of Illicit Drugs in Oral Fluid. *Appl. Spectrosc. Rev.* **2015**, *50* (9), 775-796.
- (31) Inscore, F.; Shende, C.; Sengupta, A.; Huang, H.; Farquharson, S. Detection of Drugs of Abuse in Saliva by Surface-Enhanced Raman Spectroscopy (SERS). *Appl. Spectrosc.* **2011**, *65* (9), 1004-1008.
- (32) Farquharson, S.; Shende, C.; Inscore, F. E.; Maksymiuk, P.; Gift, A. Analysis of 5-Fluorouracil in Saliva Using Surface-Enhanced Raman Spectroscopy. *J. Raman Spectrosc.* **2005**, *36* (3), 208-212.
- (33) Mostowtt, T.; McCord, B. Surface Enhanced Raman Spectroscopy (SERS) as a Method for the Toxicological Analysis of Synthetic Cannabinoids. *Talanta* **2017**, *164* (November 2016), 396-402.

H. Publications

1. Mostowtt, T.; Munoz, J.; McCord, B. An evaluation of monovalent, divalent, and trivalent cations as aggregating agents for surface enhanced Raman spectroscopy (SERS) analysis of synthetic cannabinoids, *Analyst*, **2019**, *accepted*.
2. Deriu, C.; Paudyal, J.; Bhardwaj, V.; McCord, B. SERS for the Toxicological Screening of Drugs. In *Surface-Enhanced Raman Spectroscopy: Methods, Analysis and Research*; Bhardwaj, V.; McGoron, A., Eds.; Nova Science Publishers: New York, NY, **2019**; 141-163.
3. Deriu, C.; Conticello, I.; Mebel, A.M.; McCord, B. Micro solid phase extraction surface-enhanced Raman spectroscopy (μ -SPE/SERS) screening test for the detection of the synthetic cannabinoid JWH-018 in oral fluid, *Analytical Chemistry*, **2019**, *91*(7), 4780-4789.
4. Mostowtt, T.; McCord, B. Surface Enhanced Raman Spectroscopy (SERS) as a Method for the Toxicological Analysis of Synthetic Cannabinoids, *Talanta*. **2017**, *164*, 396-402.

I. Webinars

1. Deriu, C.; Mebel, A. M.; McCord, B. The determination of synthetic cannabinoids in oral fluid using Surface-enhanced Raman spectroscopy (SERS). In *Navel Forensic Chemistry Research from Early-Career Scientists*, Webinar, September 19, 2018; Forensic Technology Center of Excellence (FTCoE).

J. Presentations

1. McCord, B. The Application of Surface Enhanced Raman Spectroscopy for the Rapid Screening of Cannabinoids and Other Drugs in Toxicological Matrices. PITTCON 2019 Conference and Expo, Philadelphia, PA, March 2019
2. Deriu, C.; Conticello, I.; Mebel, A.M.; McCord, B. Understanding the feasibility of a SERS-based screening tool for synthetic cannabinoids in oral fluid. PITTCON 2019 Conference and Expo, Philadelphia, PA, March 2019
3. Deriu, C.; Conticello, I.; Mebel, A.M.; McCord, B. SERS-based Screening Tool for Synthetic Cannabinoids in Oral Fluid. NIJ Session at PITTCON Conference and Expo 2019, Philadelphia, PA, March 2019
4. McCord, B. Detection of cannabinoids using surface enhanced Raman spectroscopy, AnalytiX 2018, Miami, FL, March 2018
5. Deriu, C.; Conticello, I.; McCord, B. SERS-based screening test for synthetic cannabinoids in oral fluid. 70th Annual Meeting of the American Academy of Forensic Sciences (AAFS), Seattle, WA, February 2018 *and* International Forensic Research Institute (IFRI) Annual Symposium, Miami, FL, May 2018 *and* American Chemical Society Florida Section (FLACS/FAME) 2018, Palm Harbor, FL, May 2018
6. McCord, B. The Application of Surface Enhanced Raman Spectroscopy for the Determination of Synthetic Cannabinoids in Oral Fluid, Emirates Forensic Conference, Dubai, UAE April 2018
7. McCord, B. Development of a Surface Enhanced Raman Spectroscopy (SERS) Method as an Alternative Method for Toxicological Drug Screening, Netherlands Forensic Institute, Amsterdam, The Netherlands, September 2016
8. McCord, B. The application of surface enhanced Raman spectroscopy in toxicological analysis, McMasters University, Hamilton, Ontario, Canada, April 2017
9. Mostowtt, T.; Deriu, C.; Munoz, J.; McCord, B. The Evaluation of Mono-, Di-, and Trivalent Cations for the Optimized Surface-Enhanced Raman Spectroscopy (SERS) Enhancement to Detect Synthetic Cannabinoids in Biological Samples. 69th Annual Meeting of the American Academy of Forensic Sciences (AAFS), New Orleans, LA, February 2017 *and* International Forensic Research Institute (IFRI) Annual Symposium, Miami, FL, May 2017
10. Deriu, C.; McCord, B. Tailored SERS-Active Substrate for Forensic Trace Detection. PITTCON 2017 Conference and Expo, Chicago, IL, February 2017
11. Mostowtt, T.; McCord, B. The Application of Gold Nanoparticles for the Trace Detection of PINACAs in Urine by Surface Enhanced Raman Spectroscopy (SERS). 68th Annual Meeting of the American Academy of Forensic Sciences (AAFS), Las Vegas, NV, February 2016 *and* International Forensic Research Institute (IFRI) Annual Symposium, Miami, FL, March 2016
12. McCord, B. Microfluidics and Nanotechnology in Forensic Science, George Washington University, Washington DC, June 2015
13. Mostowtt, T.; Doctor, E.; McCord, B. The development of surface enhanced Raman spectroscopy as a method for toxicological drug screening. International Forensic Research Institute (IFRI) Annual Symposium, Miami, FL, March 2015
14. Mostowtt, T.; McCord, B. Surface-Enhanced Raman Analysis of Synthetic Cannabinoids Using Gold Nanoparticles and Various Aggregating Agents. 67th Annual Meeting of the American Academy of Forensic Sciences (AAFS), Orlando, FL, February 2015 *and* FIU GSAW Scholarly Forum, Miami, FL, April 2015. (third place finish)